Dosimetry for Two modes of Resonance-based Wireless Power Transfer System

SangWook Park, EunHa Kim
ICT convergence team, EMI/EMC R&D Center
Korea Automotive Technology Institute
Cheonan, Korea
parksw@katech.re.kr

Kanako Wake, Soichi Watanabe
Electromagnetic Compatibility Laboratory, Applied Electromagnetic Research Institute
National Institute of Information and Communications Technology
Tokyo, Japan
kana, wata@nict.go.jp

***Abstract*—Dosimetry for the two resonant modes of resonance-based wireless power transfer system is investigated and compared. We present the physical mechanism for the two resonant modes with the simulated results and the equivalent circuit models for the wireless power transfer system. The difference between the two resonant modes for the specific absorption rate induced in the head model is discussed by comparing the electromagnetic fields for each mode.**

Keywords— dosimetry; resonance-based wireless power trasnfer; specific absorption rate; two resonant modes

I. INTRODUCTION

The concern about usage of wireless power transfer (WPT) technology have been increasing for wireless charging mobile electronics, electric vehicles and so on. It is necessary to investigate the human safety from the electromagnetic field energies generated from such systems because the very strong electromagnetic fields are radiated as compared to those used in wireless communications. Our attention here is paid to comparison of dosimetry for the two resonant modes in the resonance-based WPT system [1]. The related foundational studies have been conducted in [2]-[4].

In this paper, the comparison of dosimetry for the two resonant modes is discussed in detail. First, the physical mechanism about the two resonant modes is described with the simulation results and the equivalent circuit models. The difference of the magnitude and distribution of SAR for each mode is discussed by comparing the fields for the two modes.

II. SIMPLIFIED WPT SYSTEM

We designed a simplified WPT system consisting of two helix coils as shown in Fig 1. These helix coils play a role of resonators. The source is directly feeding at the center of the helix coil (port 1) and the other side (port 2) is terminated with the load of 50 Ω. The helix coils of 300-mm radii and 50-mm heights have 5 turns. The calculation was conducted with the full-wave electromagnetic simulation solver based on the finite integration technique (CST). The power transfer efficiency

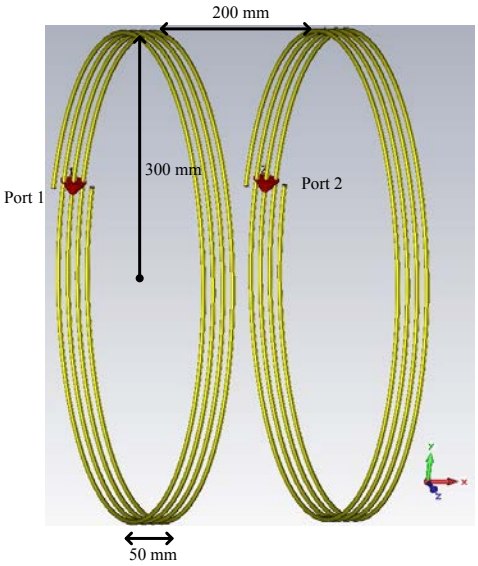

Fig. 1. Configureation of simplified wireless power transfer system.

($|S_{21}|^2$) is about 98% at the resonant frequency 9.72 MHz when the distance between the two helix coils is 330 mm. The resonant frequency is split into the two frequencies of 9.15 MHz and 10.27 MHz and the power transfer efficiencies are about 94% and 99%, respectively, when the distance between them is 200 mm. In this model, we can find that the power transfer efficiency at higher frequency is larger than that at lower frequency.

III. TWO RESONANT MODES

The WPT system uses magnetically coupled resonance phenomenon for high energy transfer efficiency at the mid-range distance. In this resonance-based WPT system, frequency splitting is clearly visible as the distance between the two helix coils decreases [5]. The physical mechanism underlying the frequency splitting is that the coupling effect

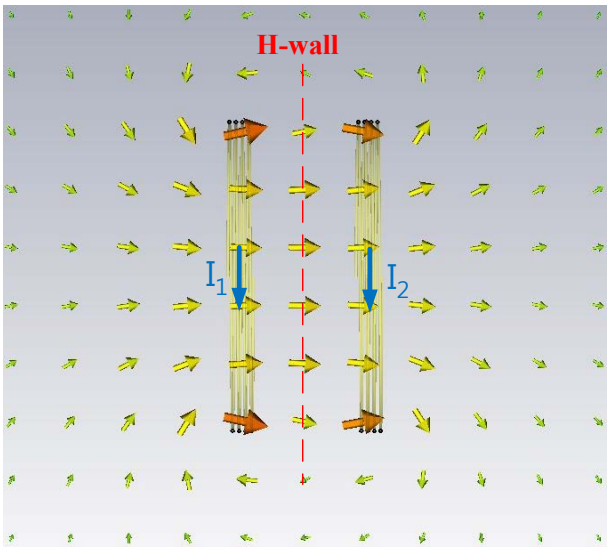

(a)

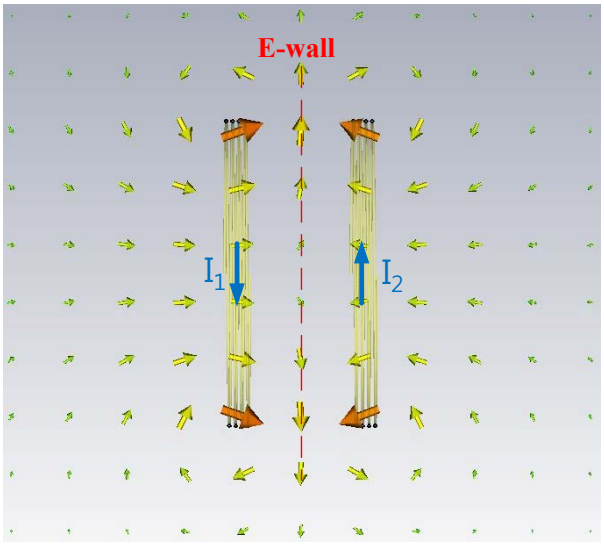

(b)

Fig. 2. Magnetic field distributions with the direction of the helix coils

can both enhance and reduce the stored energy. It has been pointed out that the frequency splitting in association with the two resonance modes can be observed if the coupled resonator circuit is over-coupled, which occurs when the corresponding coupling coefficient is larger than a critical value amounting to 1/Q, with Q the quality factor of the resonator circuit [6]. It is quite easy to confirm the two split resonant frequencies in our calculated model. Fig. 2 shows the magnetic field distributions

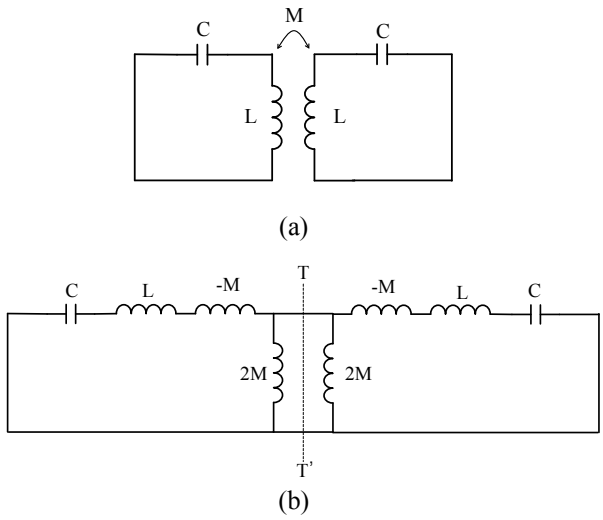

Fig. 3. Equivalent circuit of the resonance-based WPT system exhibiting the magnetic coupling. (b) An alternative form of the equivalent circuit with an impedance inverter $K = \omega M$ to represent the coupling.

with the direction of the two helix coils currents at the two resonance frequencies. At the lower resonance frequency (9.15 MHz), the two helix coils currents flow in the same direction, which constructs the magnetic wall at the center plane between the two helix coils. In the other hand, at the higher resonance frequency (10.27 MHz), the opposite direction of the two helix coils currents gives rise to construct the electric wall at the center plane between them.

For the fundamental mode near its resonance, an equivalent lumped-element circuit model is not considering any loss for the coupling structure in Fig. 1 is given in Fig. 3 (a), where L and C are the self-inductance and self-capacitance so that $1/\sqrt{LC}$ equals the angular resonant frequency of uncoupled resonators, M represents the mutual inductance. According to the network theory [7] an alternative form of equivalent circuits in Fig. 3 (a) can be obtained and is shown in Fig. 3 (b). This form yields the same two-port parameters with those of the circuit of Fig. 3 (a), but it is more convenient for our discussions. Actually, it can be shown that the magnetic coupling between the two resonant helix coils is represent by an impedance inverter $K = \omega M$.

If the symmetry plane T-T' in Fig. 3 (b) is replaced by a magnetic wall (or an open-circuit), the resultant single resonant circuit has a resonant frequency

$$f_e = \frac{1}{2\pi\sqrt{(L+M)C}}. \quad (1)$$

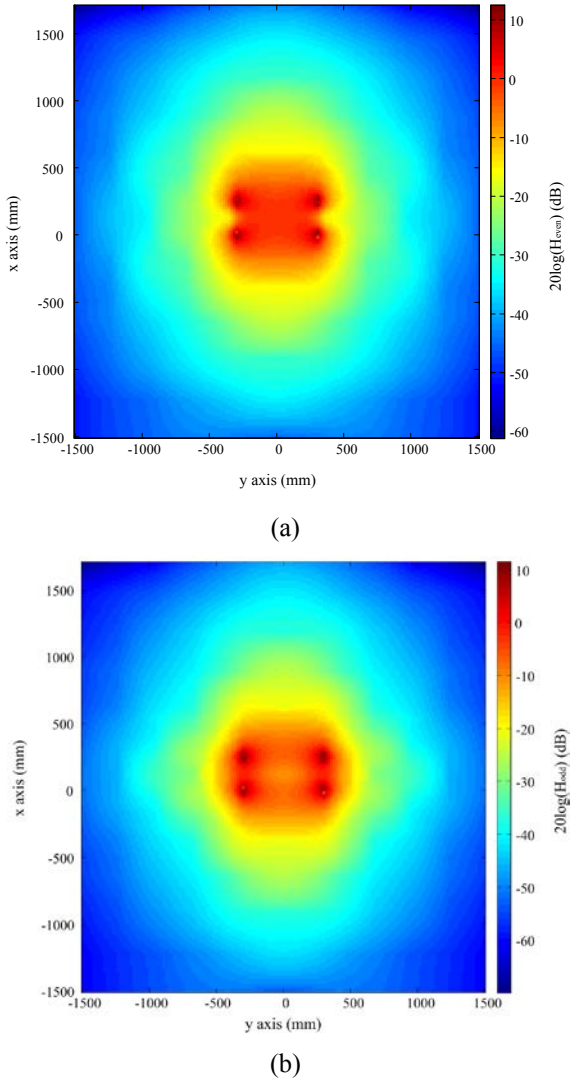

Fig. 4. Magnitude distributions of magnetic field strength at (a) lower resonant frequency (even mode) and (b) higher resonant frequency (odd mode).

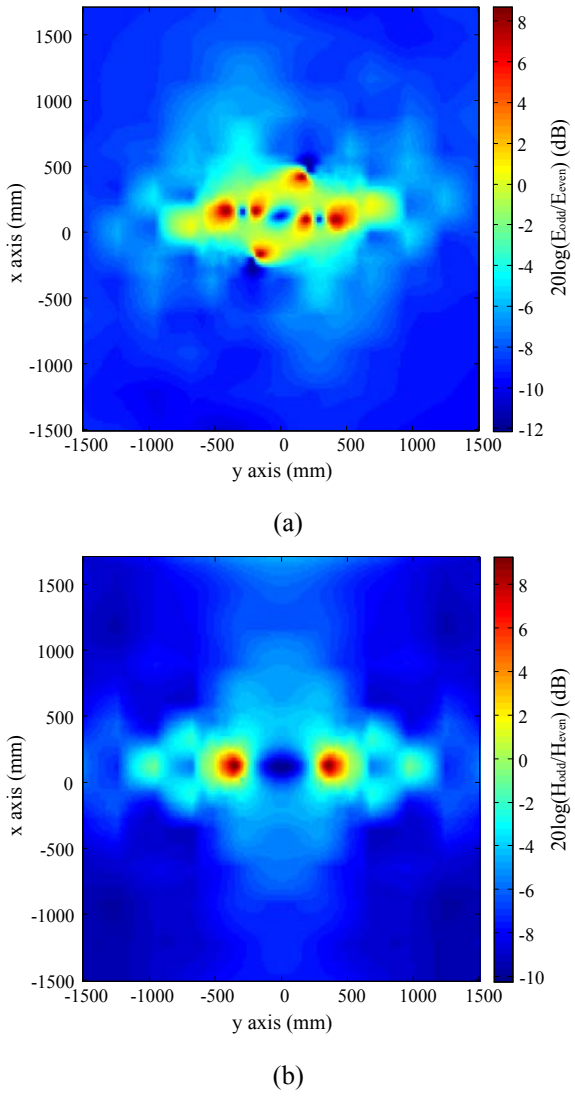

Fig. 5. Distributions of the ratio of odd-mode field strength to even-mode field strength: (a) electric field and (b) magnetic field.

This resonant mode is called "even mode" in this paper. The resonant frequency is lower than that of uncoupled single resonator, which is also confirmed in our calculation model. A physical explanation is that the coupling effect increases the stored flux in the single resonator circuit when the magnetic wall is inserted in the symmetrical plane of the coupled structure. Similarly, replacing the symmetrical plane in Fig. 3 (b) by an electric wall (or a short-circuit) results in a single resonant circuit having a resonant frequency

$$f_o = \frac{1}{2\pi\sqrt{(L-M)C}}. \tag{2}$$

We call this resonant mode "odd mode" in this paper. In this case the coupling effect reduces the stored flux so that the resonant frequency is increased.

Equations (1) and (2) can be used to find the electric coupling coefficient k

$$k = \frac{f_o^2 - f_e^2}{f_o^2 + f_e^2} = \frac{M}{L} \tag{3}$$

which is identical with the definition of ratio of the coupled magnetic energy to the stored energy of uncoupled single resonator.

IV. Comparison to Electromagnetic Field Strength for Two Resonance Modes

Fig. 4 shows magnitude distributions of magnetic field strength for the two resonant modes. As you can see the different magnetic field vector distributions for the two resonant modes in the previous section, the magnitudes of magnetic field strength distribution for the two resonant modes are also different. To compare the electromagnetic field strength for the two resonant modes, spatial distributions for the ratio of

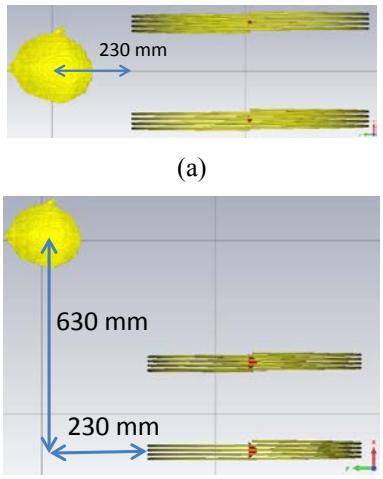

Fig. 6. Position of calculated model with respective to a WPT system: (a) Case 1 (close from the WPT system) and (b) Case 2 (far from the WPT system).

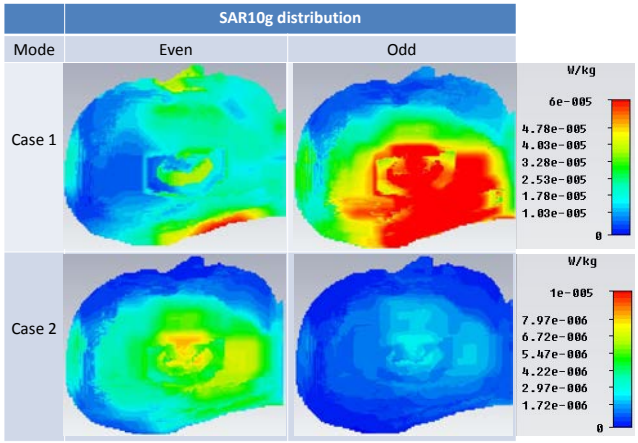

Fig. 7. Surface distributionof SAR induced in the TARO head model.

electromagnetic field strength of odd mode to that of even mode are shown in Fig. 5. From the results, we see that the electromagnetic field strength of odd mode is stronger than that of even mode in very near area from the two helix coils while that is a contrast to the former case in far area from the two helix coils despite the different the power transfer efficiency of the two resonant modes.

V. Comparison to Dosimetry for Two Resonance Modes

We have conducted the dosimetry with CST for each resonant mode of the WPT system. The head model of TARO[8] was used clearly to compare the two SAR results for each mode. The SARs were calculated for two cases: the head model situated nearby the two helix coils (Case 1) and that situated far from the two helix coils (Case 2) as shown in Fig. 6. The SAR results for the head model are listed in TABLES I.

TABLE I. SARs induced in the Head Model of TARO

	Case 1		Case 2	
mode	***Even***	***odd***	***Even***	***Odd***
SAR[a] (μW/kg)	12.9	22.1	2.1	0.7
SAR10g[b] (μW/kg)	65.7	97.5	14.5	4.1
SAR1g[c] (μW/kg)	106.5	153.8	21.5	18.4

[a.] Whole-head SAR.

[b.] Local SAR averaged over 10 g of tissue.

[c.] Local SAR averaged over 1 g of tissue.

All SARs for odd mode are larger than those for even mode in the Case 1 (the model located nearby the helix coils) while those are reverse in the Case 2 (the model located far from the helix coils) for both models. These results correspond with the relative field strength of the two resonant modes as shown in Fig. 5. The surface distributions of SAR10g induced in the TARO head model for modes and cases are shown in Fig. 7. The same tendency for the magnitude of SARs can be also identified in these results. We see that the distributions for each mode are different in Case 1. It is because the directions and magnitudes of magnetic field vectors for the two resonant modes are different.

VI. Conclusions

We have compared the dosimetry of the resonance-based WPT system for the two resonant modes. The physical mechanism about the two resonant modes (even and odd modes) of the resonance-based WPT system has been described. We have shown the difference of the fields for the two resonant modes, which gives rise to the different SARs for each resonant mode.

References

[1] A. Kurs, A. Karalis, R. Moffatt, J. D. Joannopoulos, P. Fisher, and M. Soljacic, "Wireless power transfer via strongly coupled magnetic resonances," *Science*, vol. 317, no. 5834, pp. 83-86, Jul. 2007.

[2] H. Hirayama, T. Ozawa, Y. Hiraiwa, N. Kikuma, and K. Sakakibara, "A consideration of electro-magnetic-resonant coupling mode in wireless power transmission," *IEICE Elec. Exp*. Vol. 6, No. 19, pp. 1421-1425, 2009.

[3] D. Sekine, and M. Taki, "Relationship between Human Exposure and Resonance Mode of Wireless Power Transfer with Magnetic Resonance," *IEICE Conf*., p B-4-8, 2012 (Japanese).

[4] A. Hirata, F. Ito, and I. Laakso, "Confirmation of quasi-static approximation in SAR evaluation for a wireless power trasnfer system," *Phys. Med. Biol*., vol. 58, pp. N241-N249, 2013.

[5] A. P. Sample, D. A. Meyer, and J. R. Smith, "Analysis, Experimental Results, and Range Adaptation of Magnetically Coupled Resonators for Wireless Power Transfer," *IEEE Trans. Ind. Electron*., vol.58, no. 2, pp. 544-554, Feb. 2011.

[6] B. I. Bleaney and B. Bleaney, Electricity and Magnetism, 3rd ed. Oxford: Oxford Univ. Press, 1976.

[7] C. G. Montgomery, R. H. Dicke, and E. M. Purcell, Principles of Microwave Circuits, New York: McGraw-Hill, 1948.

[8] T. Nagaoka, and et al., "Development of realistic high-resolution whole-body voxel models of Japanese adult males and females of average height and weight, and application of models to radio-frequency electromagnetic field dosimetry," Phys. Med. Biol., vol. 49, pp. 1–15, Jun. 2004.